Experimental Evidence for Quantum Tunneling Time

Nicolas Camus, Enderalp Yakaboylu,* Lutz Fechner, Michael Klaiber, Martin Laux, Yonghao Mi, Karen Z. Hatsagortsyan,† Thomas Pfeifer, Christoph H. Keitel, and Robert Moshammer‡
Max-Planck-Institut für Kernphysik, Saupfercheckweg 1, 69117 Heidelberg, Germany
(Received 20 January 2017; published 14 July 2017)

The first hundred attoseconds of the electron dynamics during strong field tunneling ionization are investigated. We quantify theoretically how the electron's classical trajectories in the continuum emerge from the tunneling process and test the results with those achieved in parallel from attoclock measurements. An especially high sensitivity on the tunneling barrier is accomplished here by comparing the momentum distributions of two atomic species of slightly deviating atomic potentials (argon and krypton) being ionized under absolutely identical conditions with near-infrared laser pulses (1300 nm). The agreement between experiment and theory provides clear evidence for a nonzero tunneling time delay and a nonvanishing longitudinal momentum of the electron at the "tunnel exit."

DOI: 10.1103/PhysRevLett.119.023201

Modern short-pulse lasers generate electric fields that are comparable in strength to those that electrons experience in atoms [1]. Effectively distorting the Coulomb potential of the atomic core, these fields allow ionization of the system with the electron tunneling through the potential barrier [2] (Fig. 1). While the tunneling ionization is of great interest to understand and describe the general quantum mechanical tunneling process [3], it is also at the heart of attosecond spectroscopy techniques. Once ionized the electron is subsequently driven by the laser field leading to various processes, such as high harmonic generation [4,5] or laser induced electron diffraction [6,7]. The resolution of attosecond spectroscopy depends essentially on our ability to understand and describe accurately the under-the-barrier dynamics of the electron at the onset of strong field tunneling ionization. Experimentally resolving electron dynamics with attosecond precision requires first to control the laser pulses on the same time scale and second to monitor with high resolution their interaction with matter [8–12].

To specifically probe the tunneling step one takes advantage of the fact that with close-to-circularly polarized laser pulses (attoclock configuration), and, therefore, a rotating electric field, the instant of time when the electron appears in the continuum is effectively mapped onto a characteristic emission direction that can be measured after the pulse [3,13–15] (Fig. 1). In order to correctly disentangle the tunneling step information (time, momentum, and position right after tunneling) in the final photoelectron momentum distribution, and to achieve a meaningful quantitative interpretation of attoclock results, the laser pulse parameters must be known and the Coulomb interaction with the remaining ion along the electron excursion in the continuum must be taken into account. At present, we are witnessing an ongoing debate about the role of the initial electron momentum [16–21] as well as the question whether and how the electron motion can be traced back to the tunneling step [14,22], whether the tunneling delay time exists [23,24], and if yes, which definition of the tunneling delay time precisely predicts attoclock experiments [15,25].

In our approach the tunneling dynamics is described quantum mechanically for a quasistatic barrier via the solution of the Schrödinger equation. For a full description of the electron dynamics in the laser field, we connect the tunneling step to the following electron excursion in the continuum which is quasiclassical already at a few de Broglie wavelengths away from the tunnel exit. The connection of the quantum and classical dynamics is carried out employing the concept of the dominant quantum path. The latter in the full quantum domain is calculated from the quantum mechanical propagator and corresponds to the most probable path connecting two space points. In the classical domain the dominant quantum path coincides with the classical trajectory, and in a consistent way determines the initial conditions of the classical trajectory in the continuum. Moreover, the initial conditions of the classical trajectory include a time delay, as

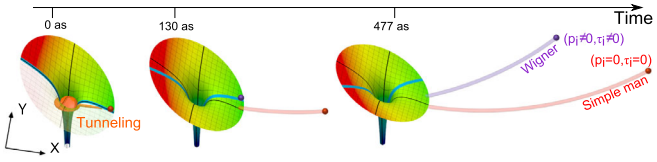

FIG. 1. Schematic representation of the ionization picture: the Coulomb potential is bent by the laser electric field forming a saddle in the potential (blue line). The bound electron wave packet is ionized through tunneling and appears as a classical particle at the tunnel exit. Depending on the initial conditions of the particle, the momentum p_i at appearance of the electron in the continuum with the time delay τ_i, different trajectories arise and appear with different momentum on the detector: the simple-man model (red trajectory) and the case where the initial conditions are given by the Wigner formalism (purple trajectory).

well as a respective momentum (Fig. 1). In this way the signatures of the tunneling step are imprinted in the asymptotic photoelectron momentum distribution.

The theoretical predictions are compared with the experiment, where a high sensitivity on the tunneling step is achieved by measuring strong-field tunneling ionization of atomic species with slightly different ionization potentials, but under otherwise absolutely identical laser and experimental conditions. To achieve this, we simultaneously collect within the same experiment photoelectron momentum distributions with high resolution for ionization of a gas mixture containing argon and krypton. Elliptically polarized, 60 fs laser pulses (1300 nm) at various intensities in the 10^{14} W/cm^2 range are focused into the gas beam at the center of a reaction microscope [26] that allows for the coincident detection of electron-ion pairs created by ionization of Ar or Kr atoms. The electron spectra of both species are separated unambiguously by means of ion tagging allowing comparison with each other.

Rather than the absolute value of the most probable photoelectron emission angle we analyze the angle difference between both targets in comparison with theory. This quantity is found to be most sensitive to the initial conditions of the electron trajectory right after tunneling, and, at the same time, almost insensitive to systematic errors or any other experimental deficiencies.

For the first step we consider the propagation of the electron's wave function, originating from the initial bound state $\Psi(\boldsymbol{r}_i, 0)$, by the space-time propagator $K(\boldsymbol{r}, \boldsymbol{r}_i, t)$ (atomic units $m_e = \hbar = e = 1$ are used throughout):

$$\Psi(\boldsymbol{r}, t) = \int d\boldsymbol{r}_i K(\boldsymbol{r}, \boldsymbol{r}_i, t)\Psi(\boldsymbol{r}_i, 0). \quad (1)$$

From the infinite number of contributing trajectories from $\boldsymbol{r}_i$ to $\boldsymbol{r}$, we identify the most dominant one. We use a quasistatic description of the laser field which is justified due to the large value of the laser period with respect to the characteristic time in the tunneling regime, described by the smallness of the Keldysh parameter [2]. In this case the electron passes the potential barrier with an almost constant energy. Accordingly, generalizing the well-known formalism introduced by Wigner [27], the most dominant path along the tunneling channel $t_W(x)$ is determined by the phase of the fixed-energy propagator $G(x, x_i, \epsilon)$. In fact, the spacetime propagator that connects the space points x and x_i in a time interval t,

$$K(x, x_i, t) = \frac{i}{2\pi}\int_{-\infty}^{\infty} d\epsilon G(x, x_i, \epsilon)e^{-i\epsilon t}, \quad (2)$$

will be maximal at the stationary phase condition $t - \partial \arg[G(x, x_i, \epsilon)]/\partial\epsilon = 0$. Taking into account that $|G(x, x_i, \epsilon)|$ is peaked at $\epsilon = -I_p$, the dominant path (Wigner trajectory) is derived:

$$t_W(x) = \left.\frac{\partial \arg[G(x, x_i, \epsilon)]}{\partial\epsilon}\right|_{\epsilon=-I_p}, \quad (3)$$

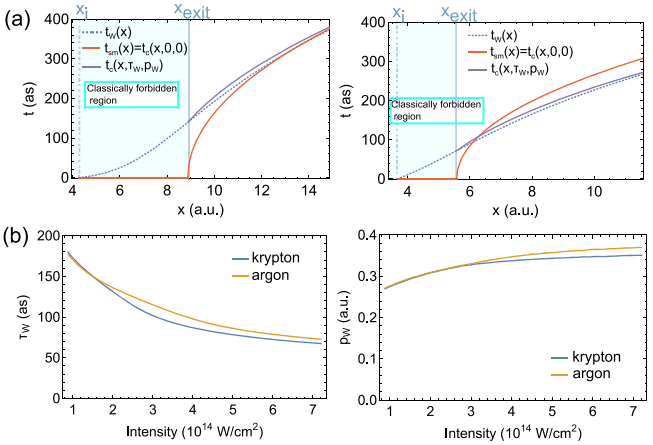

FIG. 2. (a) Electron trajectories in different models at low (left panel) and high (right panel) laser intensities: Wigner trajectory via Eq. (3) (blue dashed line), the simple-man trajectory (red solid line), classical trajectory with the initial conditions given by the Wigner formalism (purple solid line). The trajectories are calculated for a krypton atom. The laser intensities are $I = 1.7$ (left) and $I = 6.1 \times 10^{14}$ W/cm^2 (right). The trajectories are shown in one-dimensional (along the tunneling direction) Cartesian coordinate. (b) Initial conditions arising from the Wigner formalism for the two investigated atoms (argon and krypton): initial time (left panel) and initial longitudinal momentum (right panel). Notably, at the tunnel exit, the differences between both targets, argon and krypton, are as small as 10 attoseconds for the time delay and less than 0.1 a.u. for the longitudinal momentum.

where I_p is the atomic ionization potential including the Stark shift in the laser field, $x \equiv \hat{\boldsymbol{n}} \cdot \boldsymbol{r}$ is the one-dimensional tunneling coordinate with $\hat{\boldsymbol{n}}$ being the unit vector along the tunneling channel found in the parabolic coordinates, x_i is the starting point of the Wigner trajectory at time $t_0 = 0$, corresponding to the peak of the laser electric field, and $\arg[G(x, x_i, \epsilon)] = S(x, \epsilon) - S(x_i, \epsilon)$ with $S(x, \epsilon)$ being the phase of the wave function of the stationary Schrödinger equation, which is solved numerically in the parabolic coordinates (see details in the Supplemental Material [28]).

Two exemplary Wigner trajectories are shown in Fig. 2(a). They both manifest that for the most probable trajectory the electron appears at the tunnel exit x_{exit} not instantaneously but with a time delay $\tau_W \equiv t_W(x_{\text{exit}}) > 0$. Moreover, we predict a nonvanishing longitudinal momentum along the laser field direction with which the electron appears in the continuum: $p_W = [dt_W(x)/dx]^{-1}|_{x=x_{\text{exit}}}$. The value of these parameters are decisive for the interpretation of the attoclock measurement and are heavily discussed [3,15,17–19,22,23]. In our approach, both the time delay and the initial momentum are inherently provided by the Wigner trajectory $t_W(x)$. With increasing laser intensity, resulting in an effective shortening of the barrier, the tunneling time delay decreases and the longitudinal momentum becomes larger [Fig. 2(b)].

The Wigner trajectory coincides with a certain classical trajectory a few de Broglie wavelengths away from the

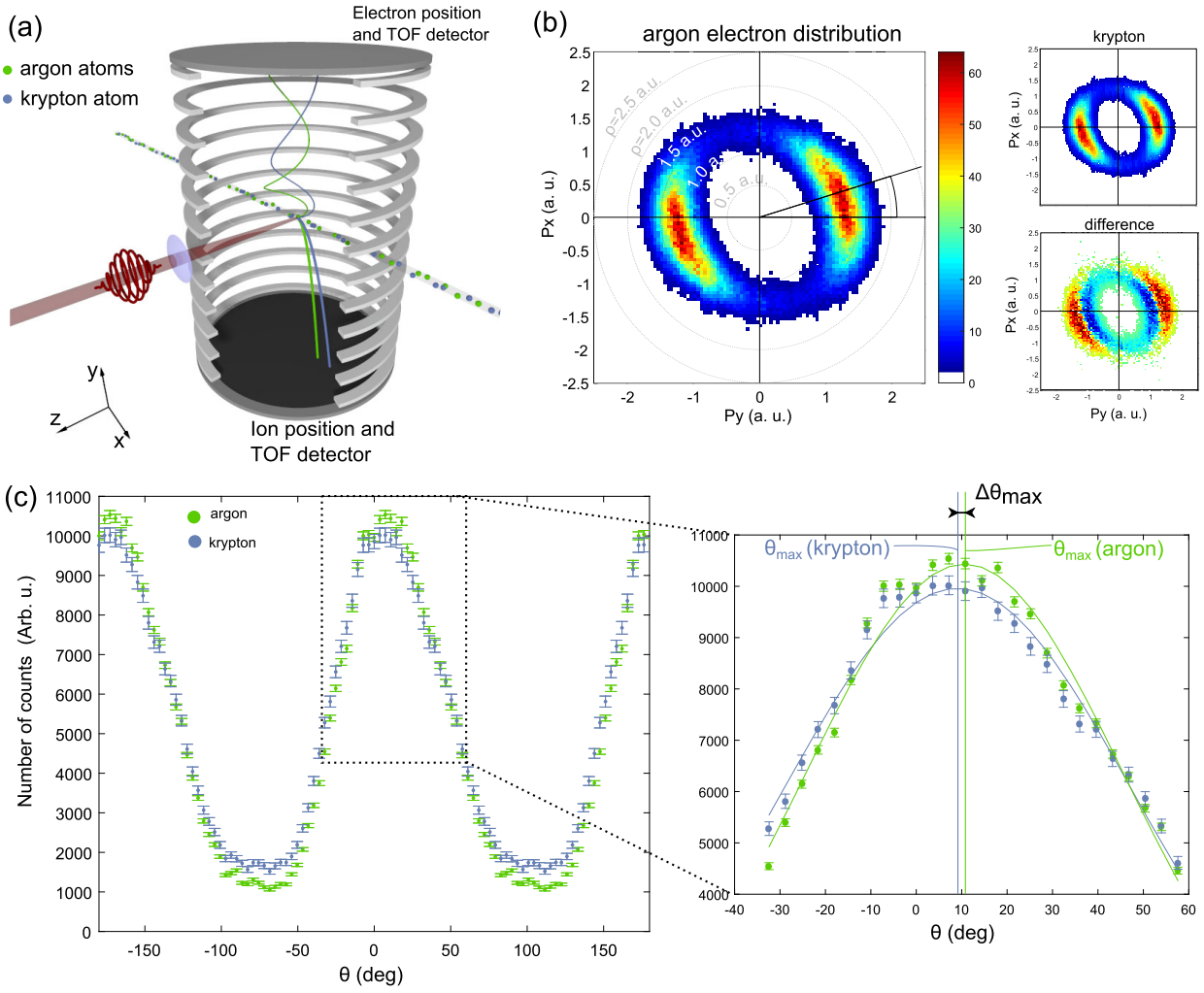

FIG. 3. (a) Sketch of the experimental setup: close to circularly polarized laser pulses with a 1300 nm wavelength are focused onto a gas mixture of argon and krypton inside a reaction microscope. (b) Experimental momentum distribution obtained when selecting the argon ionization events (left panel) or krypton (top right panel). The difference between the normalized distributions is indicated (bottom right). (c) Representation of the number of counts as a function of the θ angle for both distributions from which we extract $\theta_{\max}$ the angle at which the number of counts is maximum.

tunnel exit. However, the classical trajectory starting at the tunnel exit x_{exit} at time $t_{\text{exit}} = \tau_W$ with an initial momentum $p_{\text{exit}} = p_W$ mimics the Wigner trajectory [Fig. 2(b)] and provides the connection of the tunneling step with the subsequent electron motion in the classically allowed region. As the laser field rotates during the tunneling time delay, the electron emission direction as well as the position of the tunnel exit are adapted to the field direction after the time delay τ_W. The final electron momentum after the laser pulse is calculated via classical propagation

$$\boldsymbol{p}_f = \boldsymbol{p}_{\text{exit}} - \int_{t_{\text{exit}}}^{\infty} dt\{\boldsymbol{E}(t) + \boldsymbol{\nabla} U[\boldsymbol{r}(t)]\}, \tag{4}$$

by solving Newton's equations of motion $\ddot{\boldsymbol{r}}(t) = -\boldsymbol{\nabla} U[\boldsymbol{r}(t)] - \boldsymbol{E}(t)$, with $\boldsymbol{E}(t)$ being the laser electric field and $U(\boldsymbol{r})$ the potential of the atomic core taking into account its polarization by the laser [43].

The influence of the initial conditions on the asymptotic electron momentum is illustrated in Fig. 2(a) by comparing the Wigner trajectory $t_W(x)$ with the trajectory of the commonly used classical simple-man (SM) model $t_{\text{SM}}(x)$ where the electron appears instantaneously at the tunnel exit with an initial momentum which is equal to zero. Neglecting the atomic Coulomb potential in the SM model leads to the final momentum $\boldsymbol{p}_f = -\int_{t_0}^{\infty} dt\boldsymbol{E}(t)$. Accordingly, the additional time delay τ_W manifests as a rotation of the asymptotic momentum distribution by $\delta\theta_\tau = \omega\tau_W$, and the nonzero initial momentum to a counter-rotation by $\delta\theta_p \approx -p_w/p_E$ with $p_E = E_0/\omega$, with ω and E_0 being the laser-field frequency and amplitude, respectively. At low intensities both effects compensate each other almost completely and the corresponding trajectories merge [Fig. 2(a) left panel]. This explains, to a large extent, the success of the classical SM model in

predicting the correct electron momentum [19]. However, with increasing intensity the Wigner time delay decreases faster than the initial momentum increases leading to an additional net rotation compared to the SM prediction $\delta\theta = \delta\theta_\tau - \delta\theta_p$ [Fig. 2(a) right panel]. In the latter case, when the initial nonvanishing momentum of the electron near the tunnel exit is overlooked, the final photoelectron momentum distribution may be explained only with a negative time delay near the tunnel exit [23]. However, the physical relevant initial conditions for the classical trajectories are provided by the dominant quantum path, which points to the positive time delay near the tunnel exit, along with the initial nonvanishing momentum.

To demonstrate the relevance of the initial parameters (τ_W, p_W) and their influence on the final momentum distribution, we utilize their strong dependence on the width of the tunneling barrier.

We compare the theoretical predictions with experimental electron spectra for two atomic species with slightly different ionization potentials I_p. The data for both targets were collected within the same experiment for absolutely identical laser and experimental conditions [Fig. 3(a)]. By choosing a gas mixture of argon ($I_p^{\mathrm{Ar}} = 15.76$ eV) and krypton ($I_p^{\mathrm{Kr}} = 13.99$ eV), two species with similar physical and chemical properties, we can experimentally probe the barrier width and effectively reduce the influences of other effects such as differences in Stark shifts, atom polarizabilities or dependences on the initial-state orbital momentum [16] (see Supplemental Material [28]).

Laser pulses with a wavelength of 1300 nm and an ellipticity of 0.85 ± 0.05 have been employed. By variation of the laser intensity a detailed investigation over a large range of effective tunneling barrier widths becomes possible.

Measured electron momentum distributions for argon and krypton are shown in Fig. 3(b) at a laser intensity of about 2×10^{14} W/cm^2. As expected for atoms with similar ionization potentials, the spectra for both targets appear almost identical. However, clear differences manifest after the subtraction of the normalized distributions [Fig. 3(b)]. For comparison with theory, as mentioned above, the value of interest is the most probable electron trajectory, in particular the final momentum and the angle of rotation with respect to the axes of the polarization ellipse [13]. The latter we associate with the angle θ_{max} of the distribution where the number of counts is maximum. The angle θ_{max} is the observable that is most sensitive to both time delay and initial momentum. It is obtained from a Gaussian fit to the experimental angular distribution in range from $-50°$ to $+50°$ [Fig. 3(c)].

Instead of analysing the absolute emission angles for both targets, which would require a very precise determination of the orientation of the polarization ellipse, we concentrate on the orientation independent angle difference $\Delta\theta_{\mathrm{max}} = \theta_{\mathrm{max}}^{Ar} - \theta_{\mathrm{max}}^{Kr}$ and follow its behavior as a function of intensity. Again, to circumvent the notorious difficulties in determining the laser intensity with high accuracy, we use instead of not well determined experimental intensities the average electron momentum at θ_{max} for ionization of argon: $\rho(\theta_{\mathrm{max}}) = \rho^{Ar}(\theta_{\mathrm{max}}) = \sqrt{p_x^{\mathrm{Ar}}(\theta_{\mathrm{max}})^2 + p_y^{\mathrm{Ar}}(\theta_{\mathrm{max}})^2}$. For circularly and elliptically polarized pulses this average momentum $\rho(\theta_{\mathrm{max}})$ is an unambiguous measure of the actual intensity, in which the correct mapping from momentum to intensity must be provided by theory [44,45]. Finally, we plot $\Delta\theta_{\mathrm{max}}$ as a function of $\rho(\theta_{\mathrm{max}})$ and compare with our theoretical model (Fig. 4).

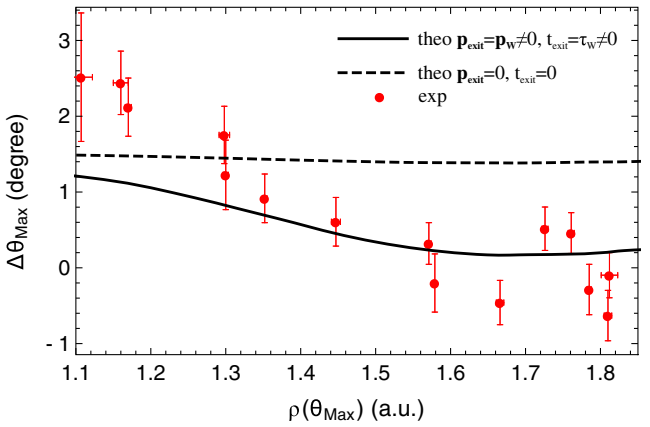

FIG. 4. Experiment and theories (with and without initial momentum and tunneling delay time). Note that the indicated tunneling theory is not fully applicable to the first three data points where the intensity is in the intermediate tunneling-multiphoton regime.

For a conclusive comparison two additional contributions, that are unavoidable in any experiment, must be considered: the focal volume averaging and the depletion effects. The theoretical curves for two sets of initial parameters are shown in Fig. 4, the solid line is for the initial conditions given by the Wigner formalism, and the dashed curve for the standard conditions (simple-man model) of zero time delay and zero initial momentum. The first observation is that—as expected—the initial conditions influence the final angle difference. Second, our results demonstrate that the simple-man model fails in reproducing subtle features in strong field ionization, which are very well reproduced with a more refined theory based on the Wigner formalism. The agreement with experiment remains even when varying in our model all possible parameters such as ellipticity, pulse duration, and pulse shape (see Supplemental Material [28]). There is no convincing way to explain the current experimental result without the initial longitudinal momentum and the time delay.

Finally, we note that the theoretical formalism presented here can also satisfactorily reproduce the previously reported experimental result of Ref. [14] (see Supplemental Material [28]). With our approach, a positive

ionization time delay and an initial nonvanishing longitudinal momentum yield the correct observed asymptotic momentum. Furthermore, the formalism naturally explains the appearance of negative ionization time delays in the analysis presented in Ref. [23], where a zero longitudinal momentum at the tunnel exit was assumed. Hence, agreement with the exact numerical simulation is achieved only if negative tunneling delay times are used as start parameters for the classical propagation Eq. (4) (see Supplemental Material [28]).

In conclusion, we have addressed the time-resolved dynamics of the tunneling ionization of an atom. We identified theoretically the tunneling delay time and the initial longitudinal momentum at the tunnel exit for the most probable trajectory of the tunneling electron and tested it experimentally. The experimental results can be satisfactorily reproduced only when these two parameters are included in the theoretical model resulting in a nonvanishing tunneling time.

N. C., E. Y., L. F., M. K., K. H., T. P., C. K., and R. M. designed the experiment. N. C., L. F., T. P., and R. M. built the experimental apparatus. N. C., L. F., M. L., and Y. M. conducted the experiments. N. C., L. F., M. L., Y. M., T. P., and R. M. performed the experimental data analysis. E. Y., M. K., K. H., and C. K. conducted the theoretical analysis. N. C., E. Y., K. H., and R. M. wrote major parts of the manuscript. All authors contributed to the interpretation and discussion of the results and commented on the manuscript.

N. C. and E. Y. contributed equally to this work.

*IST Austria (Institute of Science and Technology Austria), Am Campus 1, 3400 Klosterneuburg, Austria.
†karen.hatsagortsyan@mpi-hd.mpg.de
‡robert.moshammer@mpi-hd.mpg.de

[1] T. Brabec and F. Krausz, Rev. Mod. Phys. **72**, 545 (2000).
[2] L. V. Keldysh, Zh. Eksp. Teor. Fiz. **47**, 1945 (1964) [Sov. Phys. JETP **20**, 1307 (1965)].
[3] P. Eckle, A. N. Pfeiffer, C. Cirelli, A. Staudte, R. Dörner, H. G. Muller, M. Büttiker, and U. Keller, Science **322**, 1525 (2008).
[4] P. B. Corkum and F. Krausz, Nat. Phys. **3**, 381 (2007).
[5] F. Calegari, G. Sansone, S. Stagira, C. Vozzi, and M. Nisoli, J. Phys. B **49**, 062001 (2016).
[6] M. Meckel, D. Comtois, D. Zeidler, A. Staudte, D. Pavičić, H. C. Bandulet, H. Pépin, J. C. Kieffer, R. Dörner, D. M. Villeneuve, and P. B. Corkum, Science **320**, 1478 (2008).
[7] C. I. Blaga, J. Xu, A. D. DiChiara, E. Sistrunk, K. Zhang, P. Agostini, T. A. Miller, L. F. DiMauro, and C. D. Lin, Nature (London) **483**, 194 (2012).
[8] M. F. Kling, C. Siedschlag, A. J. Verhoef, J. I. Khan, M. Schultze, T. Uphues, Y. Ni, M. Uiberacker, M. Drescher, F. Krausz, and M. J. J. Vrakking, Science **312**, 246 (2006).
[9] D. Shafir, H. Soifer, B. D. Bruner, M. Dagan, Y. Mairesse, S. Patchkovskii, M. Y. Ivanov, O. Smirnova, and N. Dudovich, Nature (London) **485**, 343 (2012).
[10] X. Xie, S. Roither, D. Kartashov, E. Persson, D. G. Arbó, L. Zhang, S. Gräfe, M. S. Schöffler, J. Burgdörfer, A. Baltuška, and M. Kitzler, Phys. Rev. Lett. **108**, 193004 (2012).
[11] C. Ott, A. Kaldun, P. Raith, K. Meyer, M. Laux, J. Evers, C. H. Keitel, C. H. Greene, and T. Pfeifer, Science **340**, 716 (2013).
[12] D. G. Arbó, C. Lemell, S. Nagele, N. Camus, L. Fechner, A. Krupp, T. Pfeifer, S. D. López, R. Moshammer, and J. Burgdörfer, Phys. Rev. A **92**, 023402 (2015).
[13] P. Eckle, M. Smolarski, P. Schlup, J. Biegert, A. Staudte, M. Schöffler, H. G. Muller, R. Dörner, and U. Keller, Nat. Phys. **4**, 565 (2008).
[14] A. N. Pfeiffer, C. Cirelli, M. Smolarski, D. Dimitrovski, M. Abu-samha, L. B. Madsen, and U. Keller, Nat. Phys. **8**, 76 (2012).
[15] A. S. Landsman, M. Weger, J. Maurer, R. Boge, A. Ludwig, S. Heuser, C. Cirelli, L. Gallmann, and U. Keller, Optica **1**, 343 (2014).
[16] I. Barth and O. Smirnova, Phys. Rev. A **84**, 063415 (2011).
[17] A. N. Pfeiffer, C. Cirelli, A. S. Landsman, M. Smolarski, D. Dimitrovski, L. B. Madsen, and U. Keller, Phys. Rev. Lett. **109**, 083002 (2012).
[18] M. Li, Y. Liu, H. Liu, Q. Ning, L. Fu, J. Liu, Y. Deng, C. Wu, L.-Y. Peng, and Q. Gong, Phys. Rev. Lett. **111**, 023006 (2013).
[19] E. Yakaboylu, M. Klaiber, and K. Z. Hatsagortsyan, Phys. Rev. A **90**, 012116 (2014).
[20] M. Klaiber, K. Z. Hatsagortsyan, and C. H. Keitel, Phys. Rev. Lett. **114**, 083001 (2015).
[21] M. Li, J.-W. Geng, M. Han, M.-M. Liu, L.-Y. Peng, Q. Gong, and Y. Liu, Phys. Rev. A **93**, 013402 (2016).
[22] H. Ni, U. Saalmann, and J.-M. Rost, Phys. Rev. Lett. **117**, 023002 (2016).
[23] L. Torlina, F. Morales, J. Kaushal, I. Ivanov, A. Kheifets, A. Zielinski, A. Scrinzi, H. G. Muller, S. Sukiasyan, M. Ivanov, and O. Smirnova, Nat. Phys. **11**, 503 (2015).
[24] M. Klaiber, E. Yakaboylu, H. Bauke, K. Z. Hatsagortsyan, and C. H. Keitel, Phys. Rev. Lett. **110**, 153004 (2013).
[25] T. Zimmermann, S. Mishra, B. R. Doran, D. F. Gordon, and A. S. Landsman, Phys. Rev. Lett. **116**, 233603 (2016).
[26] J. Ullrich, R. Moshammer, A. Dorn, R. Dörner, L. P. H. Schmidt, and H. Schmidt-Böcking, Rep. Prog. Phys. **66**, 1463 (2003).
[27] E. P. Wigner, Phys. Rev. **98**, 145 (1955).
[28] See Supplemental Material at http://link.aps.org/supplemental/10.1103/PhysRevLett.119.023201 for details on the experimental setup, the calculations, and how the laser parameters are determined in the calculations, which includes Refs. [29–42].
[29] V. De Jesus, A. Rudenko, B. Feuerstein, K. Zrost, C. Schröter, R. Moshammer, and J. Ullrich, J. Electron Spectrosc. Relat. Phenom. **141**, 127 (2004).
[30] I. A. Ivanov and A. S. Kheifets, Phys. Rev. A **89**, 021402 (2014).

[31] The simple-man theory has been proposed about 30 years ago in different variations by several authors, see M. Yu. Kuchiev, Pis'ma Zh. Eksp. Teor. Fiz. **45**, 319 (1987) [JETP Lett. **45**, 404 (1987)]; H. B. van Linden van den Heuvell and H. G. Muller, in *Multiphoton Processes*, edited by S. J. Smith and P. L. Knight (Cambridge University Press, Cambridge, England, 1988); T. F. Gallagher, Phys. Rev. Lett. **61**, 2304 (1988); K. J. Schafer, B. Yang, L. F. DiMauro, and K. C. Kulander, Phys. Rev. Lett. **70**, 1599 (1993); P. B. Corkum, Phys. Rev. Lett. **71**, 1994 (1993), and proved to have a high predictive power in discussions of strong-field ionization phenomena.

[32] A. Becker, L. Plaja, P. Moreno, M. Nurhuda, and F. H. M. Faisal, Phys. Rev. A **64**, 023408 (2001).

[33] X. Tong and C. Lin, J. Phys. B **38**, 2593 (2005).

[34] H. G. Muller, Phys. Rev. A **60**, 1341 (1999).

[35] F. Cloux, B. Fabre, and B. Pons, Phys. Rev. A **91**, 023415 (2015).

[36] V. Shevelko and A. Vinogradov, Phys. Scr. **19**, 275 (1979).

[37] P. Schwerdtfeger, ctcp. massey. ac. nz/Tablepol2014. pdf (accessed Feb. 8, 2014) (2014).

[38] L. D. Landau and E. M. Lifshitz, *Quantum Mechanics, Course of Theoretical Physics*, edited by B. Heinemann (Oxford University Press, New York, 1981), Vol. 3.

[39] C. Z. Bisgaard and L. B. Madsen, Am. J. Phys. **72**, 249 (2004).

[40] F. W. Byron and R. W. Fuller, *The Mathematics of Classical and Quantum Physics* (Dover Publications Inc., New York, 1992).

[41] G. B. Arfken, *Mathematical Methods for Physicists* (Academic Press, New York, 2013).

[42] P. Morse and H. Feshbach, *Methods of Theoretical Physics*, International Series in Pure and Applied Physics (McGraw-Hill, New York, 1953).

[43] D. Dimitrovski, C. P. J. Martiny, and L. B. Madsen, Phys. Rev. A **82**, 053404 (2010).

[44] A. S. Alnaser, X. M. Tong, T. Osipov, S. Voss, C. M. Maharjan, B. Shan, Z. Chang, and C. L. Cocke, Phys. Rev. A **70**, 023413 (2004).

[45] R. Boge, C. Cirelli, A. S. Landsman, S. Heuser, A. Ludwig, J. Maurer, M. Weger, L. Gallmann, and U. Keller, Phys. Rev. Lett. **111**, 103003 (2013).